

Sapphire Micromachining with UV Nanosecond Lasers



CO₂ lasers have long been the laser of choice for processing applications due to their power/cost ratio. CO₂ lasers in sapphire create a classic melt pool, which can be blown out to achieve a full cut. However, the cut is often too crude for semiconductor applications. Pulsed UV lasers enable machining with much finer detail and their lack of excess heat adds another benefit: each pulse removes a small amount of material but the high repetition rate turns it into a fast process.

This paper reports how pulsed 355 nm Q-switched UV nanosecond Nd:YAG lasers with powers up to 22 W and 1.2 mJ pulse energy can successfully micromachine sapphire substrates with high accuracy and edge smoothness.

Introduction

The first supermarket barcode scanners in 1980 used polycarbonate windows, but scratches made for frequent and costly scanner unit replacement. Harder, scratch-resistant materials such as glass and sapphire soon replaced polycarbonate. High initial material growing costs plus expensive tooling kept sapphire in niche applications. However, its hardness, spectral transmission, and heat-conducting capabilities are ideal for the semiconductor industry. The proliferation of portable devices

spurred efforts to manufacture sapphire more efficiently and develop efficient methods for shaping and polishing this hard material. A recent increase in sapphire production and the associated drop in price enable new applications such as replacing chemically hardened glass or using sapphire carriers for high-powered LEDs¹. Yet its hardness challenges mechanical machining tools. Lasers provide non-contact machining with no tool wear and very high precision.

1. Shelton, Bryan. (2004) Dicing sapphire wafers. April 1, 2004, Laser Solutions.

Sapphire

Outside the manufacturing industry, sapphire is best known as a gemstone. Inclusions of trace amounts of metals give it fascinating colors. It is the third-hardest known material after diamond (C) and moissanite (SiC). Sapphire was originally grown using the Czochralski technique, and it is now typically grown using the advanced sapphire crystalline growth process (ASCGP) in boules up to 200 kg and directly in sheets using the edge defined film fed growth (EDFFG) process with wafer sizes up to 150 mm diameter².

Sapphire is highly transparent to wavelengths between 170 nm and 5.3 μm ^{3,4}. This lack of absorption complicates laser absorption in the material—there is little absorption at 355 nm. However, with pulsed lasers, it is sufficient to penetrate into the material and release the high intensity in a small volume. With nanosecond laser pulses, a mixture of thermal- and photochemical-breaking of bonds can remove small fractions of sapphire. Dosing the right amount of energy under the right angle can polish a smooth surface⁵. Ultra-short pulses stimulate nonlinear effects directly in the sapphire, often creating novel features.

As a crystal, sapphire is sensitive to light polarization and scan direction. Cutting a circle with linear polarization is faster when the polarization axis coincides with the scan direction, and circular polarization was applied in all the following experiments.

Scribing and Cutting with 30-100 ns Q-Switched Pulses at 355 nm

Laser ablation with 30 ns pulses is a thermal process. The interaction between the beam and the material starts with linear absorption of the photons. However, the high energy of 1.2 mJ pulses and excellent beam quality can create such high intensities that the process switches to a non-thermal regime. The following experiments used Lumentum Q-Series lasers, and combining photo-thermal and non-linear effects created interesting cutting results. UV interacts with twice the absorption of IR at 1064 nm⁽²⁾, and UV also focuses to a smaller spot size, enabling the machining of finer features. High photon energy can break chemical bonds directly without dissipating into heat. On the other hand, reducing the energy close to the threshold allows for a controlled, small removal rate. Typical reported values of threshold fluence are between 100 and 300 J/cm²^{6,7}.

Separating a thin sheet into two halves can be done without any tools by simply breaking it, and the break line is somewhat predictable. For precise separation, a shallow groove or scribe is cut on the surface. Transparent materials allow lasers to add a scribe or weakening line inside the material. In hard materials, applying break force along the scribe will separate the sheet in a fine, controlled manner. This technique is limited to straight lines and does not separate sections from the inside of the sheet. A full cut allows for cutting out any shape anywhere in the sheet.

There are three distinctive methods to separate sapphire:

- Surface scribing followed by snapping action
- Internal scribing followed by snapping action
- Full cut by mining a deep trench

The focus of this paper is the use of a full cut, although the results can be applied to surface scribing. Three methods are evaluated to find the best technique for a full cut of sapphire:

- Single shot in one dimension
- Line shapes in two dimensions
- Removing one surface layer and combining surface layers three-dimensionally into a full cut.

The lasers used in this evaluation were the JDSU Q-Series Q301 and Q304. The power for both lasers delivered at the work surface was 11 W. The Q301 has a pulse width of 30 ns at 10 kHz and the Q304 100 ns at 40 kHz. The divergence of 2 mRad was captured with a collimating lens to a beam diameter of 1.2 mm. Various focal diameters were obtained through a variable beam expander. The delivering focusing lens on a Hurryscan-10 galvanometer-scanner is 100 mm.

Single Shot in One Dimension

A single-shot removal involves the fewest number of processing parameters. Only the energy per pulse, the pulse width, and the beam diameter (resulting in a fluence-value) are essential. It also has a pure material interaction in the absence of the plasma plume and debris. At 10 kHz, the intensity is too high for a single shot—the surface tends to crack. For the Q304, single-shot depth was deepest at the maximum available energy of 275 μJ at 40 kHz. The reported fluence is the average energy per area.

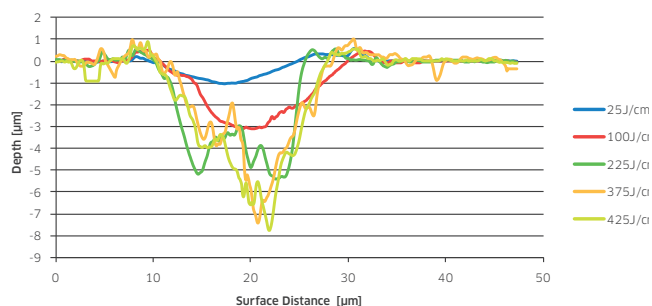


Figure 1. Cross sections of single shots vs. fluence

Figure 1 shows single-shot cross sections at various beam expander (BEX) settings at 40 kHz, 9.5 W. The width of the ablated spot remains nearly constant for all focal diameters. Figure 2 shows the recorded depths. Depth increase appears to saturate with tighter focusing. Photos also show droplet melt next to the input holes

2. Elena R. Dobrovinskaya, Leonid A. Lytvynov, Valerian Pischik. (2009) Sapphire material-products-properties. s.l.: Springer, 2009. ISBN 0387856943.
3. R. K. Route, M. M. Fejer, A. Alexandrovski and V. Kondilenko. (2004) Heat-Treatment and Optical Absorption. 2004. LIGO LSC meeting, LLO 3/17/04.
4. Takayuki Tomaru, Takashi Uchiyama, Daisuke Tatsumi, Akira Yamamoto, Takakazu Shintomi. Cryogenic measurement of the optical absorption.
5. X. Wei, X.Z. Xie, W. Hu, J.F. Huang. (2012) Polishing Sapphire Substrates by 355 nm Ultraviolet Laser. Guangzhou.
6. Patel, Ashwini Tamhankar and Rasj. (2010) Optimization of UV laser scribing process for LED sapphire wafers. LIA ICALEO, 2010. M701.
7. O. Uteza, B. Bussiere, F. Canova, J.-P. Chambaret, P. Delaport, T. Itina, M. Sentis. (2007) Laser-induced damage threshold of sapphire in nanosecond, picosecond and femtosecond regimes. Applied Surface Science, 2007, Vol. 254. 799-803.

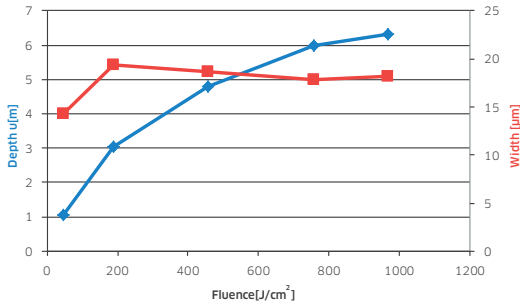


Figure 2. Depth and width vs. fluence

Pulse energy of 240 µJ with a 11 µm focal spot appear to be good starting values. The fluence (pulse energy and focus diameter) may need to be further optimized once a decent full cut has been established.

Line Shapes in Two Dimensions

To create line-shaped geometries, laser output is scanned through a galvo system. Adjusting the pulse repetition rate (PRR) versus the scan speed creates a pulse overlap leading to a solid line. Care must be taken when adjusting the overlap as the plasma plume and displaced material interferes with the next pulse. A quarter-waveplate converts the linear polarization into a circular polarization, resulting in equally efficient X and Y scanning.

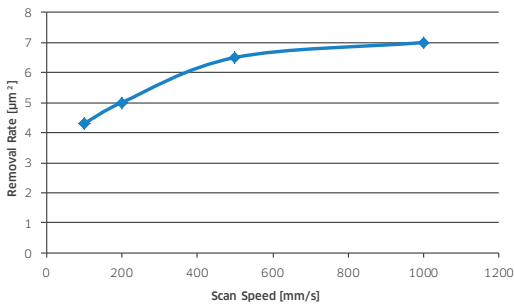


Figure 3. Sapphire removal rate at 40 kHz, 9W, 80 ns

The depth of a single scribe was measured with various scan speeds at 40 kHz and is plotted in Figure 3. The removal rate is defined as vertical cut area per 1 ms.

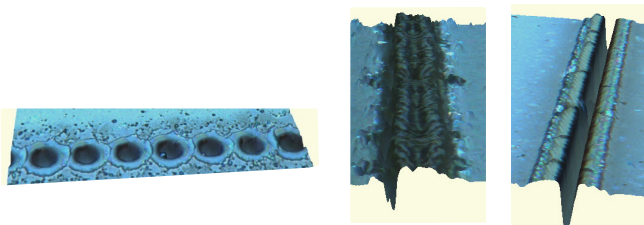


Figure 4. Low overlap, high overlap, good scribe

Figure 4 shows three different results: a low overlap resulting in individual holes, a very high overlap resulting in debris build-up that makes removal less efficient (especially for subsequent scans)⁸, and an optimum depth result with clean edges. The trend from quality to quantity scribe is from low fluence with high overlap to high fluence with low overlap. Based on Figure 3, the optimum speed for the next phase is somewhere above 500 mm/s.

Various wobble configurations and flat-top converters did not increase removal efficiency.

Removing and Combining Layers in Three Dimensions

After multiple scans on a single line, the narrow opening slows down the debris escape path. A wider channel is needed to cut deeper. A common technique is to scribe multiple lines with a defined offset. Different strategies can be applied to setting the order in which individual lines are scribed. One possible solution is to address the individual line in a linear fashion, meaning that an adjacent line will always be scribed next. This keeps debris build-up on the treated side. This build-up is easily removed and it does not seem to hamper removing the next layer. Figure 5 shows 12 parallel scribes from left to right with a line pitch of 1 µm. The material is pushed over the previous scribe with the last scribe leaving a shallow trench.

Large line pitches and slow scanning speeds result in a rougher surface. An aluminum plate under a polished sapphire sample always shows the first line marked into it. Subsequent lines (with a line-pitch less than 1 beam diameter) in a layer are not visible due the scattering nature of the entry surface. Figure 5. Debris build-up after multiple pitched lines

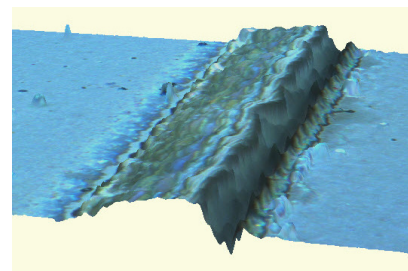


Figure 5. Debris build-up after multiple pitched lines

Several pitches from 0.5 to 10 µm in combination with a variety of scan speeds were evaluated. The scanner resolution is limited to 0.5 µm. Figure 6 shows depth after normalizing each curve to the same amount of scans to 1 µm pitch. The pulse energy was 225 µJ with a 12 µm focal diameter.

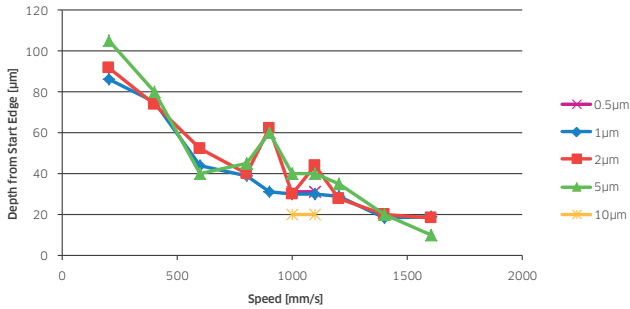


Figure 6. Normalized depth to scan speed

Figure 7 and 8 show the lowest and highest fluence comparison removal rates by adjusting the beam expander and keeping the sapphire surface at the focal plane constant. The scan speed was 1000 mm/s with 9 W at 40 kHz. This translates to 25 J/cm² with a 35 µm focused spot size and 500 J/cm² with an 8 µm focused spot size. The vertical axis is the depth per mm² surface area per second. The 25 J/cm² with >5 µm line pitch was unique, with lower efficiency. Intensities above 400 J/cm² show a strikingly constant around 30 µm/mm²/s independent of the pitch distance.

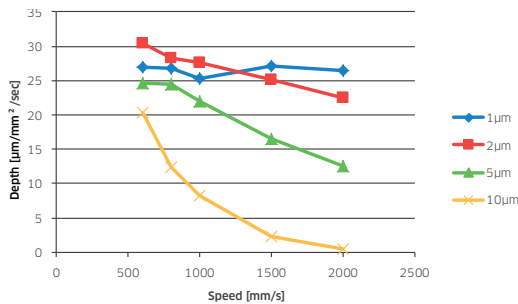


Figure 7. Fluence comparison removal rates at 25 J/cm² efficiency

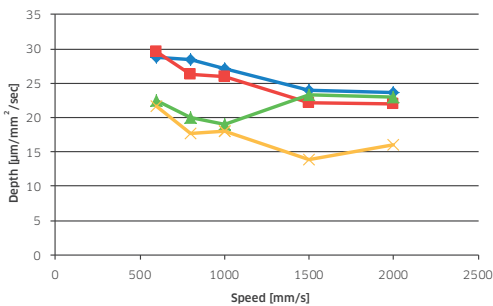


Figure 8. Fluence comparison removal rates at 500 J/cm² efficiency

Based on this data, a good parameter set is 1000 mm/s with 1 µm step size. The 1 µm pitch frees up requirements for the spot size and, with that, the overlap.

Depth vs. Power

Polarization combining two 40 kHz lasers showed a 2x reduction in time for a full cut; the curves in Figure 9 can be extrapolated up to at least 21 W. This was the case with a 180° phase delay or 80 kHz and 0° phase delay for 40 kHz and 2x pulse energy.

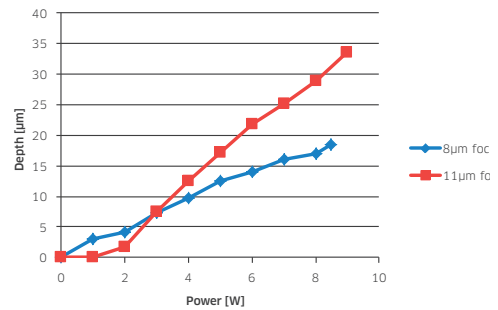


Figure 9. Depth versus applied power at 1000 mm/s, 1 µm pitch, 9 W

Focus Position Effects

Figure 10 reflects a study on focusing using a scan speed of 1000 mm/s and 1 µm line pitch. The laser was operated at 40 kHz with 9 W average output power. With a focal lens of 100 mm, the calculated average fluences in air were 25, 225, and 450 J/cm², respectively, with corresponding Rayleigh ranges (RR) of 2700, 280, and 100 µm.

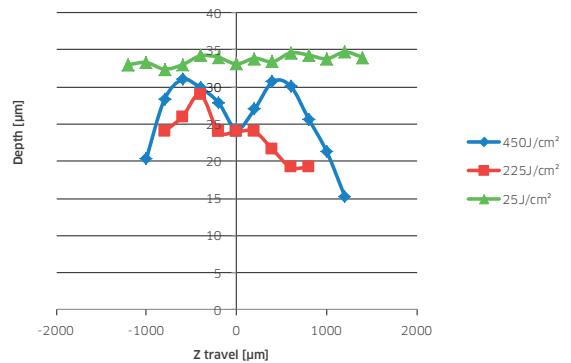


Figure 10. Focusing at 1000 mm/s, 1 µm pitch, 9 W

The green curve represents the lowest fluence, with a Rayleigh range longer than the 300 µm thick substrate. As expected, the achieved depth is independent from the focal position. The highest fluence has a Rayleigh range shorter than the substrate thickness but the tolerance to the focal position appears to be much larger than the Rayleigh range. The low fluence is preferred due to the benefit of low tolerance to the focal position.

Cutting Geometry

To study full cuts, a 5 mm diameter disc was chosen. The separating trench is generated by the galvo-scanner in a spiral pattern with transversal overlap similar to the found line pitch of 1 μm . Evaluating multiple full cuts shows that the wall taper is about 8.5. Assuming 30 μm depth per layer, it takes 10 layers to cut through the full 300 μm thickness. Calculating backward from the last single circle, then upward along the 8.5° walls, an entry width of at least 200 μm is required.

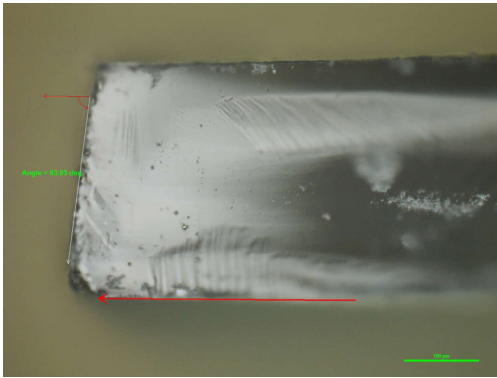


Figure 11. Wall aspect ratio

9 W produced a wall angle of about 6°. Higher powers produced steeper walls. Using a higher fluence produced better results not only by reducing the amount of cutting material with straighter walls but also by maintaining a better cutting depth.

Full Cut Result

The final goal of this study was to find the fastest way to get a full cut of a 5 mm disc. The cutting geometry described above contains $15 \cdot 10^6 \mu\text{m}^3$ per mm length. With a pulse repetition rate of 40 kHz at 1000 mm/s, 10 W, and a line pitch of 1 μm , this results in an effective cutting speed of 0.5 mm/s for a 300 μm thick sapphire substrate. With a 22 W UV source, the effective cut speed increased linearly to 1.2 mm/s. The cut duration proved to scale with the thickness squared between 200 and 1000 μm thick sapphire. Measured edge chipping was less than 3 μm and the edge surface roughness was $R_a=2.0$. No cracks were observed. The edge surface roughness is optimal at large angles between the surface and the beam⁵. Debris is easily removed with a wipe or in an ultrasonic bath.

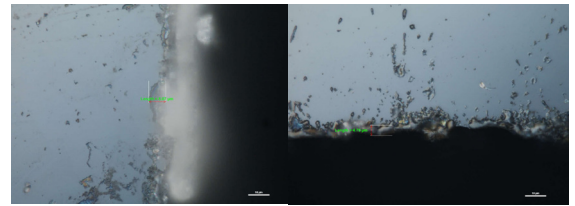


Figure 12. Left-input and right-exit edge smoothness with a 100X microscope objective

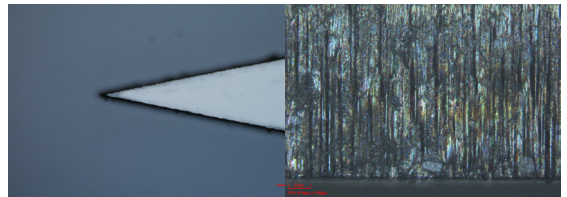


Figure 13. Point of a star cut out and edge roughness

Conclusions

We have successfully applied pulsed Q-switched UV nanosecond lasers to shape and cut sapphire substrates with high accuracy and edge smoothness. Full optimal cut parameters can be found by systematically approaching the removal rate of one-dimensional single shots by adjusting the power, pulse width, and focus diameter. With the second phase, two-dimensional line shapes are optimized by adding the parameters of speed and pulse overlap. The third, three-dimensional phase explored the addition of the line pitch and subsequently the composition of multiple scans. The optimal parameters of one phase do not necessarily transfer to the next phase, but these changes themselves show how to converge to the best solution.

The combination of 3D cutting and the galvo system can cut sapphire of any shape and a wide variety of thicknesses.



North America
Toll Free: 800 498 5378

Worldwide
Tel: +800 5378 5378
www.lumentum.com

© 2015 Lumentum
Product specifications and descriptions in this document are subject to change without notice.

sapphire-wp-cl-ae 30176032 900 0115